ARCHIVES OF ELECTRICAL ENGINEERING VOL. 63(2), pp. 139-147 (2014)

DOI 10.2478/aee-2014-0011

FE analysis of current displacement phenomena in a squirrel cage motor working at cryogenic temperature

MARIUSZ BARAŃSKI

Institute of Electrical Engineering and Electronics, Poznań University of Technology
Piotrowo 3a, 60-965 Poznań, Poland
e-mail: mariusz.baranski@put.poznan.pl

(Received: 15.11.2013, revised: 17.12.2013)

Abstract: The paper presents the special software for transient FE analysis of coupled electromagnetic-thermal problems in a squirrel cage submerged motor working at cryogenic temperature. A time-stepping finite element method and transients analysis of an induction motor has been applied. The non-linearity of the magnetic circuit, the movement of the rotor, skewed slots, and the influence of temperature on electric and thermal properties of the materials has been taken into account. Developed on the basis of presented algorithm a computer program used to analyze the phenomenon of current displacement in the rotor bars of high-voltage cage induction motor working in cryogenic conditions. The results of the simulations are presented.

Key words: FE analysis of submerged induction motor, cryogenic temperature, coupled electromagnetic-thermal phenomena, current displacement

1. Introduction

A detailed analysis of electromagnetic and thermal transients is necessary to improve the methods of induction motor design. Reliability design calculations strongly depends on the accuracy with which the applied mathematical model representation the phenomena in a considered machine. Thus, in a consideration is necessary to take a full account of the movement of the rotor, nonlinear properties of magnetic materials, influence of temperature on electric, magnetic and thermal properties of the materials, eddy-current distribution in the rotor bars and skewed slots [1-3]. This problem is especially important during the analysis and design of a special squirrel cage motor, e.g. a motor working in cryogenic conditions [1].

In [1] authors proposed algorithm and computer program for transient finite-element (FE) analysis of coupled electromagnetic-thermal problems in a squirrel-cage induction motor working at cryogenic temperature. A great influence of temperature on the change of the stator windings resistance and squirrel winding conductivity at the start-up of the motor working in

liquid nitrogen has been observed. In [13] results of the investigation of the induction motor designed for operate in cryogenic temperature have been presented. Two kinds of the investigation have been performed. At first simulation of the motor work has been carried out by solving equations of the mathematical model. At second, measurements have been done on the constructed full-scale model of motor. An analysis of the effect of the permeability of magnetic wedge material on the electromagnetic torque and phase current calculation in high voltage induction motor working in cryogenic conditions was presented in [9]. In [9, 13] calculations were carried out on the basic of computer program for the electromagnetic field analysis.

In this paper, a special software which was developed on the basis of algorithm for transient FE analysis of coupled phenomena proposed in [1] is used to analyze the phenomenon of current displacement in the rotor bars of the motor working in cryogenic conditions. The Figure 1 shows a four-pole, 3-phase, high voltage squirrel-cage motor with rating data $U_N = 6600$ V, $f = 60$ Hz, $P_N = 785$ kW. The motor is intended to work at cryogenic temperature 161°C in liquefied natural gas (LNG). In this temperature the superconductivity phenomenon does not occur. The motor is designed to drive a cargo pump when unloading an LNG carrier. The motor under our analysis was built in Poland by MIKROMA S.A. Company.

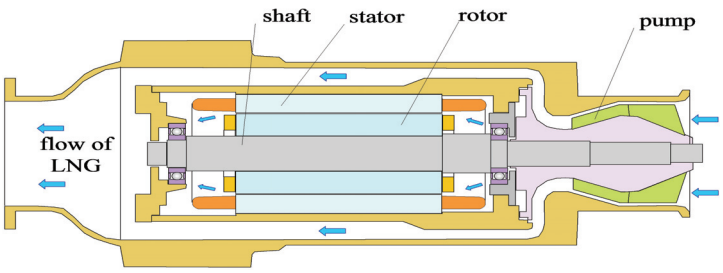

Fig. 1. Induction motor with a pump

The motor is mounted on the driving shaft of the turbine of the pump. The rotor, stator and windings are immersed in LNG. Therefore the motor is well cooled. Its characteristic feature is a large current density at rated load.

2. Mathematical model

The field-circuit approach to modeling of an induction motor has been applied to undertake the problem. The equations of the electromagnetic field have been coupled with the equations of the thermal field using the 2D finite element modeling.

In order to represent the skew of the rotor slots, the machine was cut into w disks (sections) along the z-axis parallel to the shaft. Each section concerns a different position of the rotor

with respect to the stator [1-6]. In presented model the windings segmented into elementary conductors associated with disks [4, 6]. The magnetic coupling of the disks is neglected.

The 2D representation of the edge value of magnetic vector potential **A** is used to describe the magnetic field. The edge value of **A** is defined as a product of the disk length l_w and the A_z component of **A** ($\varphi = l_w A_z$). The disks are subdivided into finite elements. The non-linear differential matrix equations describing the distribution of the magnetic field and currents in the winding may be written in the following matrix form [1]

$$\begin{bmatrix} \mathbf{S}_w + \mathbf{G}_w(\mathbf{1} - \mathbf{C}_{kw})\mathrm{p} & -\mathbf{z}_w \\ -\mathbf{z}_w^T\mathrm{p} & -(\mathbf{R} + \mathrm{p}\mathbf{L}) \end{bmatrix} \begin{bmatrix} \boldsymbol{\varphi}_w \\ \mathbf{i} \end{bmatrix} = \begin{bmatrix} \mathbf{0} \\ -\mathbf{U} \end{bmatrix}, \tag{1}$$

where $\mathbf{S}_w$ is the reluctance matrix, $\mathbf{G}_w$ is the matrix of elementary conductances associated with the edges, $\mathbf{C}_{kw}$ is the coefficients submatrices, $\mathrm{p} = d/dt$, $\mathbf{z}_w$ is the matrix that transforms the currents associated with the edges into loop currents **i**, $\boldsymbol{\varphi}_w$ is the vector of edge potentials for disk, **R** is the diagonal matrix of winding resistances, **L** is the matrix of end-turns inductances, **U** is the vector of supply voltages.

The above presented equation is coupled with thermal FE equations. These equations are written as follows [1]

$$(\mathbf{S}_\theta + \mathbf{K}_\theta + \mathbf{G}_\theta p)\theta = \mathbf{P} + \mathbf{K}_{\theta o}, \tag{2}$$

where $\mathbf{S}_\theta$ is the thermal conductivity matrix, $\mathbf{K}_{\theta b}$ and $\mathbf{K}_{\theta o}$ are the coefficients matrices describing the heat transport to the surrounding of the motor, $\mathbf{G}_\theta$ is the matrix of heat capacities, θ is the vector of nodal values of temperature, **P** is the vector of nodal heat sources. It has been assumed that there are 3 types of heat sources: (a) losses in windings, (b) eddy current losses in the cage bars, and (c) core loss. The losses (a) and (b) are determined by the current density distribution obtained from (1). The losses of category (c) are calculated for each FE using a standard technique [7, 12]. In the considered coupled problems, the windings resistance, the elements of conductances matrix and the reluctance matrix in (1) depend on the temperature. Thus $\mathbf{R} = \mathbf{R}(\theta)$, $\mathbf{G} = \mathbf{G}(\theta)$, $\mathbf{S} = \mathbf{S}(\theta)$.When determining the elements of matrices **R** and $\mathbf{G}_w$ it was taken into consideration that the resistivity ρ_θ of the copper and the conductivity σ_θ of the aluminum were calculated from well know equations [1]

$$\rho_\theta = \rho_{Cu\,20^\circ\mathrm{C}}\left(\frac{235+\theta}{235+20}\right), \tag{3}$$

$$\sigma_\theta = \sigma_{Al\,20^\circ\mathrm{C}}\left(\frac{225+20}{225+\theta}\right), \tag{4}$$

where θ is the temperature in the Celsius scale, $\rho_{Cu20^\circ\mathrm{C}}$, $\sigma_{Al20^\circ\mathrm{C}}$ are the resistivity of the copper and the conductivity of the aluminum at 20°C respectively [7, 11]. The elements of the reluctance matrix $\mathbf{S}_w$ depend on magnetic permeability of ferromagnetic materials.

Heat transfer occurs in three different modes, i.e. when temperature differences are present by conduction, convection and radiation [7]. The major heat transfer at the boundaries of the

induction motors is by conduction or convection. In the outer surface of the frame of the motor, heat is mainly transferred by convection, and the boundary condition is

$$k\frac{\partial\theta}{\partial n} = -h\left(\theta - \theta_a\right), \tag{5}$$

where k is the heat conductivity coefficient, h is the heat transfer coefficient, θ_a is the temperature of the fluid surrounding the motor.

The equations of the electromagnetic-thermal model are coupled through the electromagnetic torque T_{el} to the equation of motion,

$$J_b\frac{\mathrm{d}^2\alpha}{\mathrm{d}t^2} + T_o = T_{el}, \tag{6}$$

where J_b is the moment of inertia, α is the angular position of the rotor, T_o is the load torque. The electromagnetic torque T in Equation (6) is calculated on the basis of the magnetic field distribution.

The solution is obtained by the time-stepping method. The time discretization leads to the following system of non-linear algebraic matrix equations [1, 2]

$$\begin{bmatrix} \left[\mathbf{S}_w^n + \mathbf{G}_w(\mathbf{1}-\mathbf{C}_{kw})\Delta t^{-1}\right] & -\left[\mathbf{z}_w\right] \\ -\left[\mathbf{z}_w^T\right] & -(\mathbf{R}\,\Delta t + \mathbf{L}) \end{bmatrix} \begin{bmatrix} \left[\boldsymbol{\varphi}_w^n\right] \\ \mathbf{i}^n \end{bmatrix} = \\ = \begin{bmatrix} 0 \\ -\Delta t\,\mathbf{U}^n \end{bmatrix} + \begin{bmatrix} \left[\mathbf{G}_w(\mathbf{1}-\mathbf{C}_{kw})\Delta t^{-1}\right] & \mathbf{0} \\ -\left[\mathbf{z}_w^T\right] & -\mathbf{L} \end{bmatrix} \begin{bmatrix} \left[\boldsymbol{\varphi}_w^{n-1}\right] \\ \mathbf{i}^{n-1} \end{bmatrix}, \tag{7}$$

$$\left(\mathbf{S}_\theta^n + \mathbf{K}_{\theta b}^n + \mathbf{G}_\theta^n\,\Delta t^{-1}\right)\boldsymbol{\theta}^n = \mathbf{P}^n + \mathbf{K}_{\theta o}^n + \mathbf{G}_\theta^n\,\Delta t^{-1}\,\boldsymbol{\theta}^{n-1}, \tag{8}$$

$$J_b\left(\alpha_{n+1} - 2\alpha_n + \alpha_{n-1}\right)/\left(\Delta t\right)^2 = T_n - T_{n0}, \tag{9}$$

where n denotes the number of time-steps, Δt is the time-step length.

3. Numerical implementation

Due to the coupling existing between the amounts of electrical, mechanical and thermal Equations (7)-(9) are solved simultaneously. The solution of one of the non-linear algebraic equations containing from tens to hundreds of thousands of equations is complex and time-consuming. It gives rise to many problems e.g. numerical, software and hardware. To calculate the equations can be used typical iterative methods. However, they are usually not very effective for this type of problem. For these reasons to solve complex system of Equations (7)-(9) author is proposed a method of relaxation block. The Newton-Raphson method was

used to solve the equations of each block [8]. The electromagnetic torque has been calculated using the FE representation of the Maxwell stress tensor formula [10]. The formula has been obtained by the analysis of virtual displacement corresponding to the MBM [6].

4. Simulation results

On the basis of presented algorithm for solving the equations within the field-circuit model a computer program for simulates electromagnetic-thermal phenomena in a full-scale model of squirrel cage submerged motor was elaborated. It allows automatic generation of mesh of area concerned with the user selected software parameters such as: number of pole pairs, the number of stator and rotor windings, single or dual-layer winding, fractional slot winging, winding connection. Developed procedures used in a special computer software allow you to choose a different shapes of motor slots. Analysis of the phenomena in the considered motor can be carried out without taking into account how and when considering the skewed rotor slots. The program allows to carry out the calculations using a three-phase motor power system sinusoidal voltage as well as distorted voltages. It takes account of eddy current, the influence of magnetic field and temperature on the magnetic properties of ferromagnetic materials and the effect of temperature on conductivity and thermal conductivity materials. The results of the calculation can be visualized as a graphs, a waveforms, electromagnetic and thermal field distribution, schedules and save the file to the isotherms to further processing.

The stator and the rotor of squirrel cage motor are shown in Figure 2 [1]. The electromagnetic circuit has a mass about two times smaller than a classical motor of the same power. All elements of the motor have been tested before assembling the entire construction. It was mainly voltage and climatic tests for coils and infrared tests for core of the stator that were performed.

a) b)

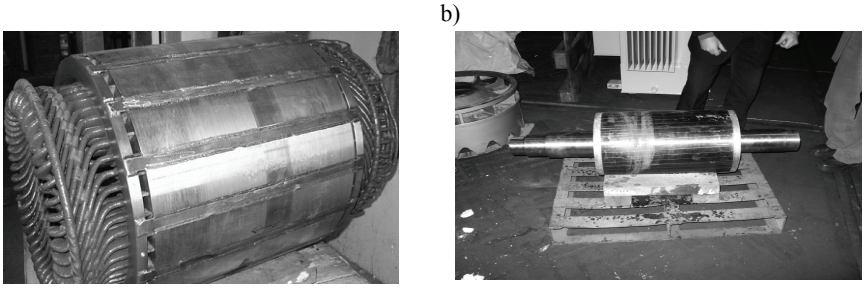

Fig. 2. Stator a) and rotor b) of a high voltage motor

Selected results of the calculations of no-load start-up of the motor operating at supply voltage decreased to 5240 V are shown in Figures 3, 5-6. The calculations were performed for the machine working in air temperature of $\theta = 20°C$ and liquid nitrogen temperature ($\theta = -196°C$). In order to obtain the best possible representation of material parameters in computations, the

characteristics B(H) of electrical sheets were measured [9]. The obtained currents time characteristics are shown in Figure 3. On the basis of the obtained calculation results we have found that the transient state caused by the start-up of the motor working at cryogenic temperature is 1.5 s and is three times longer than the start-up of the motor working at ambient temperature $\theta = 20°C$. It is caused by a smaller rotor cage resistance after the immersion of the motor in liquid nitrogen.

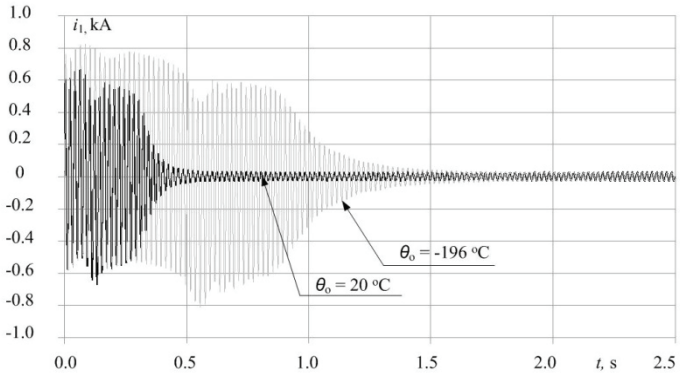

Fig. 3. Calculated phase currents waveforms at no-load start-up of the motor for $\theta = 20°C$ and $\theta = -196°C$

The calculated distributions of amplitudes of the current density j along the rotor bar height for t = 0.5 s are shown in Figures 5-6. Such a non-uniform distribution of the current density causes stronger heating of the upper part of the rotor bars. Current density distribution is shown for a few selected rotor bars – Figure 4. Due to the fact that the tested motor is axial symmetry his ¼ part was investigated.

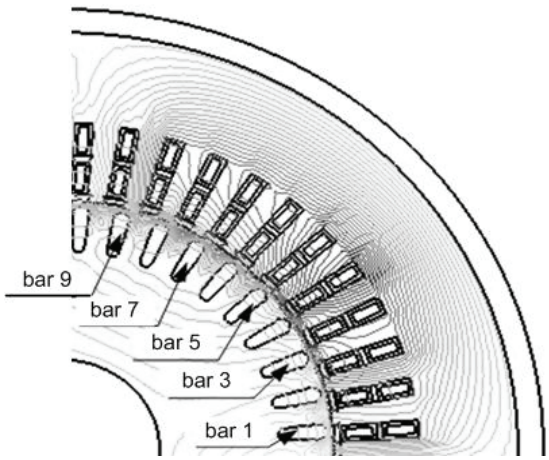

Fig. 4. Localization of the rotor bars considered

In Figures 5-6 we can observe very strong current displacement. Also shows that the current density distribution affects the position of the rotor bar relative to the stator teeth. The ratio k current density in the upper part of the rotor bar to its density in the lower part for temperature $\theta_o = 20°C$ is $k_{20} = 6.4$, and for the temperature $\theta_o = -196°C$, $k_{-196} = 11.7$. Such large displacement current in the rotor bar is caused by high conductivity of aluminum at cryogenic temperature. Due to the high current density the more heat the sub-rod on the upper part thereof. In turn, the temperature distribution effects on the conductivity distribution σ of aluminum along the rotor bar [1].

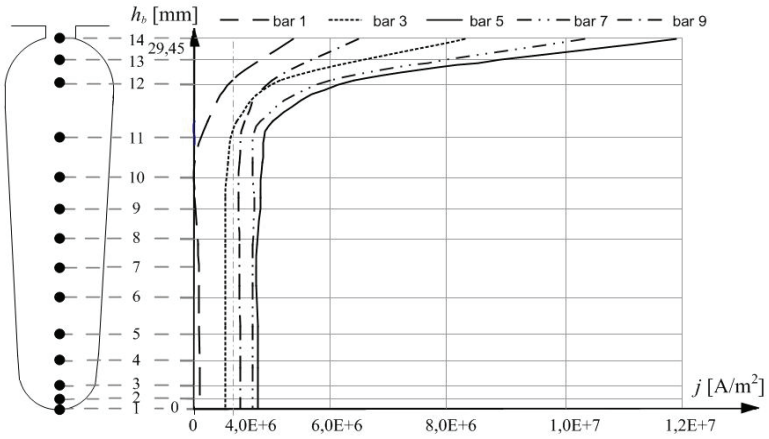

Fig. 5. Distribution of current density j along the height of the rotor bar at no-load start-up of the motor for $t = 0.5$ s; $U_s = 5240$ V; $\theta_o = 20°C$

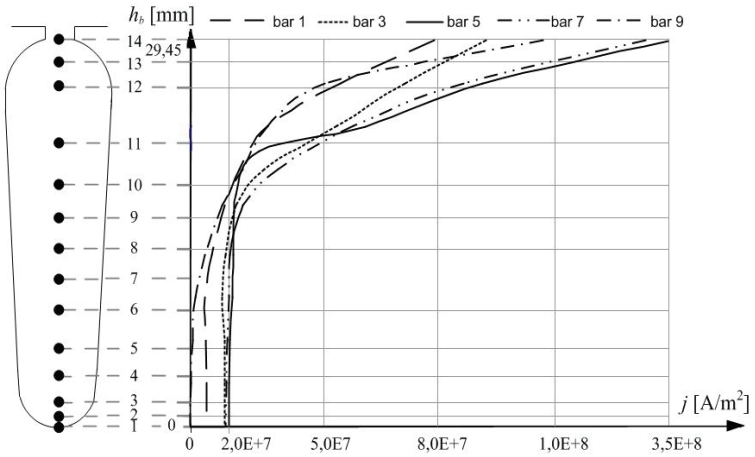

Fig. 6. Distribution of current density j along the height of the rotor bar at no-load start-up of the motor for $t = 0.5$ s; $U_s = 5240$ V; $\theta_o = -196°C$

The Figure 7 shows the distributions of the temperature increase Δθ of the aluminium along the height h_b of the selected rotor bar for t = const at no-load start-up of the motor.

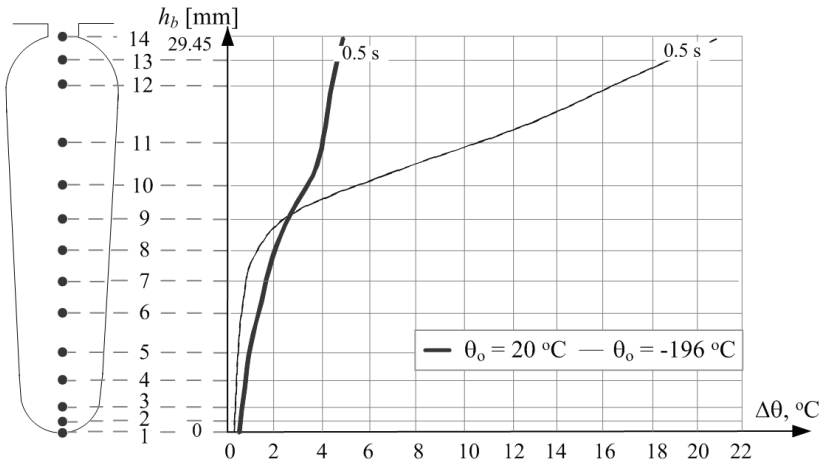

Fig. 7. Distributions of the temperature increase Δθ of the aluminum along the height hb of the selected rotor bar for t = const at no-load start-up of the motor

5. Conclusions

The presented coupled model has been successfully applied to the analysis of the influence of temperature on transients of the high voltage squirrel cage motor. It should be noted the influence of the position of the rotor bar on the current density distribution. Analyze of the current density distribution in anywhere rotor bar might suggest that all the rotor bars have the same distribution. This approach is correct, when it is a consequence of the use of simplification in the mathematical model or in focus on the current density distribution in a specially selected and specifically located rotor bar. The obtained results show that the temperature influences on the transients electromagnetic, as well as on the amplitude of the currents in steady states. A great influence of temperature on the change of the squirrel winding conductivity of the motor working in liquid nitrogen has been observed. This is due to the accumulation of factors determining the eddy-current distribution in the rotor bars, i.e. the large depth of rotor slots and a resistivity of almost eight times less than when considered at room temperature.

Acknowledgments
This project was realized under the 6th Frame Programme funded by the European Union (acronym NG2 SHIP I/F, number TST3-CT-2003-506154).

References

[1] Barański. M., Szeląg W., *Finite element analysis of transient electromagnetic-thermal phenomena in a squirrel cage motor working at cryogenic temperature.* IET Science Measurement and Technology 6(5): 1-7 (2012).

[2] Barański M., Demenko A., Łyskawiński W., Szeląg W., *Finite element analysis of transient electromagnetic-thermal phenomena in a squirrel cage motor*. COMPEL – The International Journal for Computation and Mathematics in Electrical and Electronic Engineering 30(3): 832-840 (2011).
[3] Kolondzovski Z., Belahcen A., Arkkio A., *Multiphysics thermal design of a high-speed permanent-magnet machine.* Appl. Therm. Eng. 29(13): 2693-2700 (2009).
[4] Piriou F., Razek A., *Model for coupled magnetic-electric circuits in electric machines with skewed slots*. IEEE Transactions on Magnetics 26(2): 1096-1100 (1990).
[5] Ho S.L., Fu W.N., *A comprehensive approach to the solution of direct-coupled multislice model of skewed rotor induction motors using time-stepping eddy-current finite element method*. IEEE Transactions on Magnetics 33(3): 2265-2273 (1997).
[6] Demenko A., *Movement simulation in finite element analysis of electric machine dynamics*. IEEE Transactions on Magnetics 32(3): 1553-1556 (1996).
[7] Driesen J., *Coupled electromagnetic-thermal problems in electrical energy transducers.* PhD Thesis, Faculty of Applied Science, K.U. Leuven (2000).
[8] Driesen J., Hameyer K., *Newton and quasi-Newton algorithms for non-linear electromagnetic-thermal coupled problems.* Compel 21(1): 116-125 (2002).
[9] Barański M., *Influence of the magnetic wedge materials on characteristics of 3-phase high voltage induction motor.* Archives of Electrical Engineering 56(2): 173-182 (2007).
[10] Henrotte F., Hameyer K., *Computation of electromagnetic force densities: Maxwell stress tensor vs. virtual work principle.* 168(1-2): 235-243 (2004).
[11] Flynn T.M., *Cryogenic Engineering'.* Second edition, CRC Press, New York (2005).
[12] Mezani S., Takorabet N., Laporte B. *A Combined electromagnetic and thermal analysis of induction motors*. IEEE Transactions on Magnetics 41(5): 1572-1575 (2005).
[13] Kołowrotkiewicz J., Barański M., Szeląg W., Długiewicz L., *FE analysis of induction motor working in cryogenic temperature.* COMPEL – The International Journal for Computation and Mathematics in Electrical and Electronic Engineering 26(4): 952-964 (2007).